An Overview Algorithm to Minimise Side Lobes for 2D Circular Phased Array

S. Mondal
London South Bank University; School of Engineering
103 Borough Road, London SE1 0AA

Abstract
The report presents an algorithm called the total focusing method for the circular phased array. It shows an improvement in the focusing for the main lobe beam and eliminates the effects of the side lobe. The report visualizes the effects for different ring sizes of the circular array and the effect of different numbers of array elements. The results of this modelling indicate that, for a given number of elements, placing them around the circular ring allow them to perform best and that the element spacing should be less than half a wavelength to avoid grating lobes and to eliminate grating lobes. In addition to that it describes how the TFM images have been built by computing half time traces of the transmitter and receiver array.

Keywords: Phased array, ultrasonic beam focusing and total focusing method

1. Introduction

The phased array technology is now a popular technique in the field of NDT inspections where a complex geometry is involved. The main advantages of the phased array system are of its beam steering and focusing capabilities which allows geometry to inspect areas where physical access is not possible. In recent years phased array technology has enhanced the way in which engineers evaluate components for their structural safety and protection, introducing a new form of inspection known today as phased array NDT non-destructive testing. Application of phased arrays (PA) can vary from pressure vessel testing, aerospace and nuclear power plants and further to the medical field where its application was initially implemented. The early 1970's saw the use of a PA system confined to the medical field, later introduced in the industrial industry in the 1980's, but because of varying acoustic properties, complex component geometries and ranges in material thicknesses found in industrial testing, application of PA in this field presented a greater challenge [1,2].

Due to the amount of possible element configurations experiments concluded by [6], demonstrated the effects of three different geometrical selections of elements. The visual response of the circular array designs showed the best performance in terms of beam directivity not only this, by increasing the number of elements decreases the amplitude of the grating lobes and proved to be more superior in terms of obtaining the lowest array performance indicator (API) values.

In the journal published by [4], the spherical-section produced a much higher focal intensity gain and the amplitude of the grating lobes with respect to the focus was lower when compared to planar geometries. Another method of beam focusing analysed the beam directivity and the pressure distribution to predict the behaviours of focusing oppose to steering. A numerical simulation was utilised to show some key effects of focusing within and beyond the transition range. L.Azar, Y. Shi and S-C Wooh **[3]** demonstrated a focusing method which involved a parabolic time delay; taken from the Huygens principle; propagating waves are focused to a specific point within a material where all the individual

wave fronts are summed up therefore producing maximum focal beam intensity along any desired direction.

1.1 Simulation of array data

The arrays are compared by simulating the response to a point reflector that can be located anywhere in the +z halfspace, as indicated in Figure 1. To do this time domain signals (time-traces) are simulated for every transmitter-receiver combination. For example, if n is the number of elements in the array then a maximum of n x n possible time-traces are available for all transmitter-receiver combinations. However, the number of independent time-traces that actually need to be computed for the simulation is only $\frac{n}{2}(n+1)$, because the time-trace when element 1 transmits to element 2 is identical to the time-trace when element 2 transmits to element 1 due to reciprocity. The mathematical details of the circular phased array, in term of the time traces of the transmitting and receiving signal, and frequency responses analysis is described in the journal paper [6].

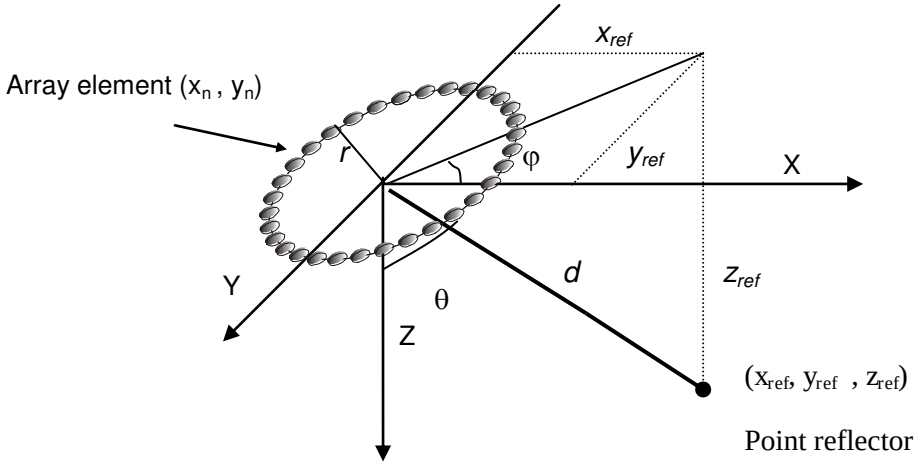

Figure 1 : Array elements are uniformly spaced on the circumference of a circle of radius, r, in the x-y plane and a point reflector is in the x-y-z plane.

1.2 Total focusing method (TFM) imaging

The synthetic aperture focusing technique (SAFT) uses only the pulse echo responses of the array so that it does not take advantage of the much larger number of responses for various pairs of elements that can be recorded with an array. The total focusing method does utilize all combinations of sending and receiving elements, also called full matrix capture, to from an image [5].

The formation of a TFM image with a circular array (Figure 1) with N elements. In this case, it has been recorded all the voltage time domain signals V(X_{tn}, X_{rm},t), (n= 1..N),(m= 1…N),

for sending element whose centroid is located at X_{tn} and a receiving element whose centroid is at X_{rm} . In the image formation process a grid of image points has been setup as shown in Figure 2, advance all these sending/receiving element pair responses by the travel times T(Xtn,Y) +T(Xrm,Y) and then calculate their sum at time t =0 to form an image, $I_{TFM}(Y)$, giving

$$I_{TFM}(Y) = \sum_{n=1}^{N}\sum_{m=1}^{N} V(X_{tn}, X_{rm}, t + T(X_{tn}, Y) + T(X_{rm}, Y))$$

Transforming the measured time domain signals to the frequency domain and evaluate at M positive frequencies, as in the SAFT method, the alternate frequency domain TFM form:

$$I_{TFM}(Y) = 2Re\left\{\frac{\Delta\omega}{2\pi}\sum_{k=1}^{M}\sum_{n=1}^{N}\sum_{m=1}^{N} V(X_{tn}, X_{rm}, \omega_k) exp[-i\omega_k T(X_{tn}, Y) - i\omega_k T(X_{rm}, Y)]\right\}$$

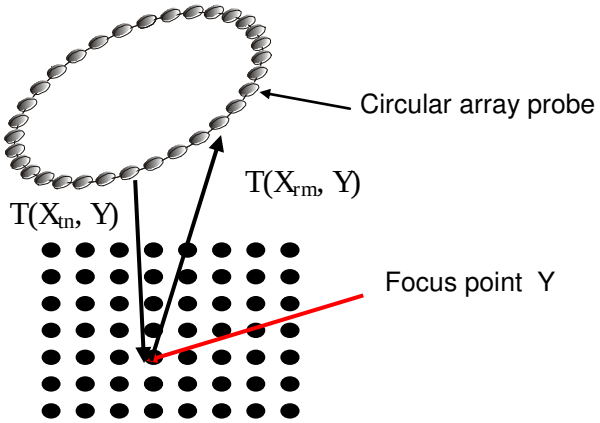

Figure 2: Imaging algorithms for the TFM scan

2 Fundamental of the TFM mapping

In the TFM mapping, each input (x, y) and output value (z) from the function corresponds to a point on a grid, the images are created corresponding to the colours on the colour bar, the lowest point is represented as dark blue; the highest point is represented as red.

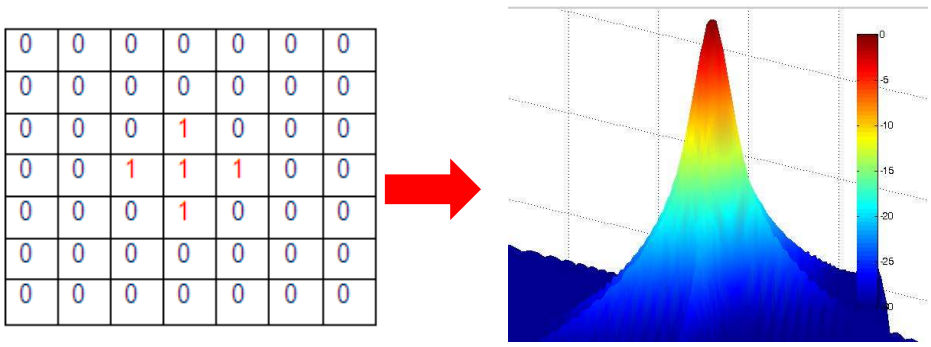

Figure 3.1: **Grid representation of beam**

In phased array simulation; the point representing the strongest focus of the beam are displayed on a grid like image as shown in Figure3.1; only the colours showing the strongest (deep red) and weakest points (dark blue) which are also demonstrated on the grid as 0 and 1 are displayed at the point above the threshold (cut-off point) removing all remaining colours in-between.

2.1 Results and Discussion

For a circular array the characteristics of the main lobe, side lobes and grating lobes are governed by geometrical parameters such as ring size, inter-element spacing, and number of elements. The effect of varying these geometrical parameters is shown in Figures 4(a)-(c) and Figures 5(a)-(c).

Figures 4(a)-(c) demonstrate the effect of varying ring diameter while the number of elements is kept constant and equal to eight. In Figure 4(a) the ring diameter is 1.67λ and the space between elements is $\lambda/2$. The result shows that there are no side or grating lobes but that the main lobe width is large. In Figure 4(b) and Figure 4(c) the ring size is increased to 3.33λ and 5λ respectively. The main beam lobe width is decreased but there are indications of grating lobes due to the space between elements being greater than $\lambda/2$. In Figures 5(a)-(c) the number of elements is increased in a circular array with a fixed diameter of 5λ. The figures show that as the number of elements increases the amplitude of the grating lobes decreases. In Figure 5(c) there are no side lobes because for 32 elements, the inter-element spacing is less than $\lambda/2$ in a 5λ diameter ring.

.

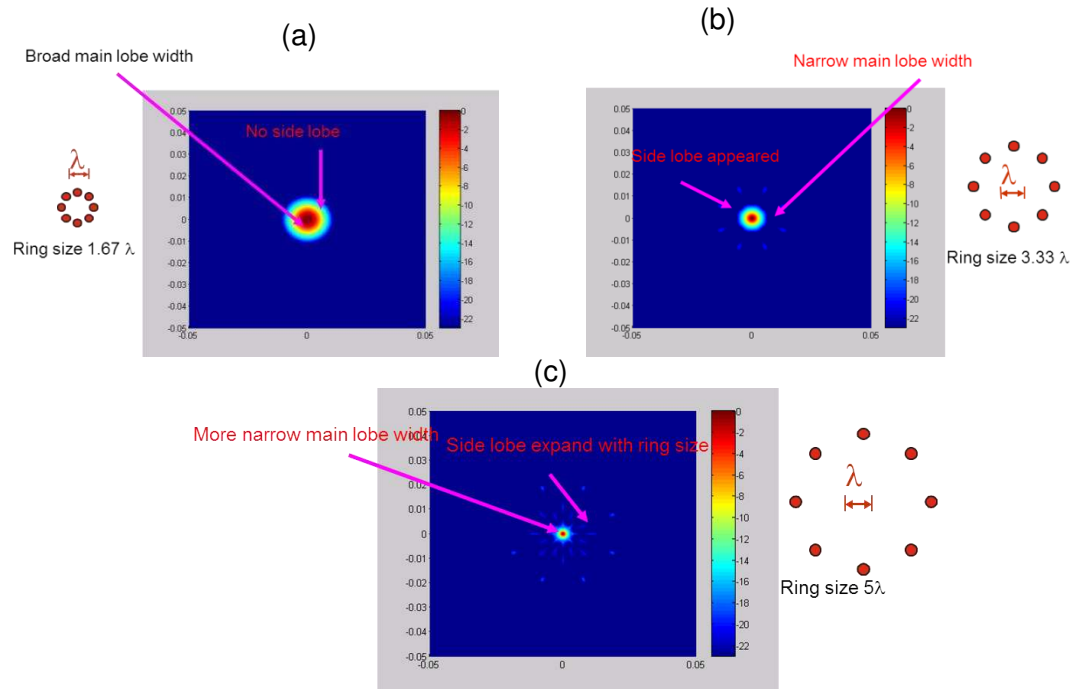

Figure 4 : Effect of ring size on side lobes and main beam width for an 8 element circular array transducer: (a) ring size 1.67 ␣␣␣␣(b) ring size 3.33 ␣; (c) ring size 5 ␣␣␣The scales shown

to right of each image are in dB.

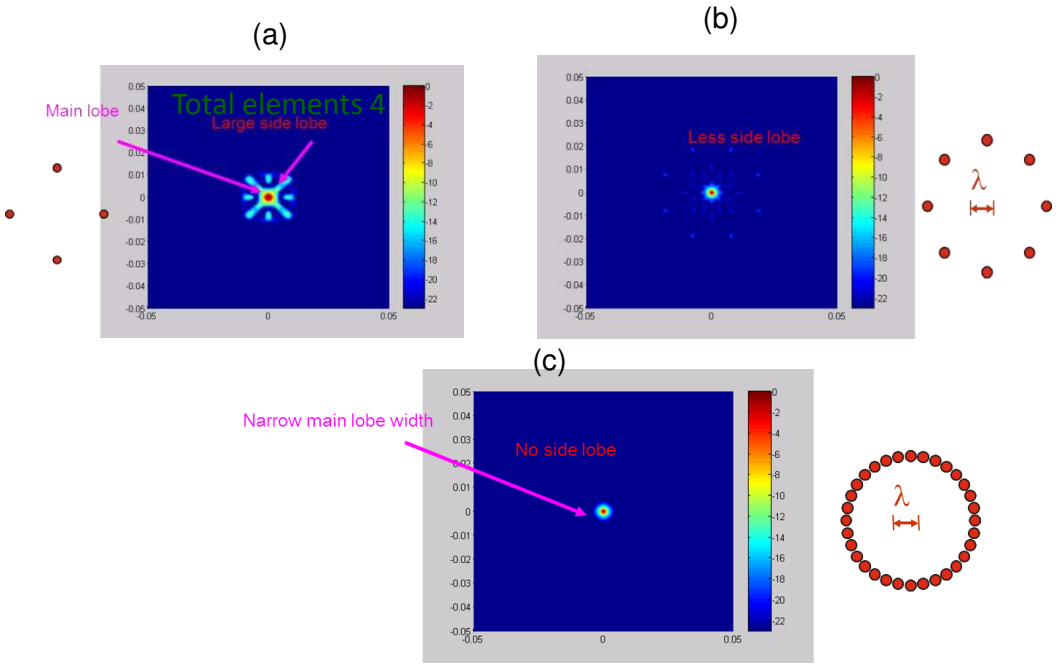

Figure 5: Effect of number of elements on side lobes when the diameter of the circular array is 5λ (a) 4 elements; (b) 8 elements; (c) 32 elements. The scales shown to right of each image are in dB.

3. Conclusions

The parameters that determine the outcome in the scanned image include the used frequency, propagation material, strength of the main lobe, transducer properties and electrical networks. It is important that for these to be carefully considered in hopes of achieving the best image resolution; an ideal outcome would show a narrowly focused, high intensity beam with minimal unwanted defects in the image such as grating and side lobes. These are unwanted abnormalities that occur in the scanned image reducing the focus of the main beam; parameters that are involved with side lobes include element configuration, frequency, the element size; number, pitch and spacing as well as the bandwidth. Grating lobes occur when the element size is equal or greater than the wavelength but no longer visible when the size is less than half a wavelength. To spot such abnormalities, concentration of the main-lobe; together with increasing intensity range of the near field delivering maximum penetration of usable focus for a given array, needs to be improved to allow greater detection.

References

[1] Yen, J.T., and Smith, S.W., 2002, "Real Time Rectilinear Volumetric Imaging," IEEE Trans. Ultrason. Ferroelectr. Freq. Control, **49,** no. 1, pp. 114-124.

[2] Mendelsohn,Y., and Wiener-Avnear, E., 2002, "Simulations of Circular 2D Phase-Array Ultrasonic Imaging Transducers," Ultrasonics, **39**, pp. 657-666.

[3] Azar, L., Shi, Y. and Wooh, S. (2000). Beam focusing behavior of linear phased arrays. NDT & E International, 33(3), pp.189-198.

[4] Ebbini, E. and Cain, C. (1991). A spherical-section ultrasound phased array applicator for deep localized hyperthermia. IEEE Transactions on Biomedical Engineering, 38(7), pp.634-643.

[5] Holmes, C., Drinkwater, B. and Wilcox, P. (2005). Post-processing of ultrasonic phased array data for optimal performance. Insight – Non-Destructive Testing and Condition Monitoring, 47(2), pp.88-90.

[6] Mondal, S., Wilcox, P. and Drinkwater, B. (2005). Design of Two-Dimensional Ultrasonic Phased Array Transducers. J. Pressure Vessel Technol., 127(3),

[7] Daniel, H.T., and Stuart, F., 1991, " Beam Steering with Pulsed 2D Transducer Arrays," IEEE Trans. Ultrason. Ferroelectr. Freq. Control, **39**, no. 4, pp. 464-475.

[8] Wooh, S.C., and Yijun, S., 1999 "Optimum Beam Steering of Linear Phased Arrays," Wave Motion, **29**, pp. 245 – 265.